

# 23. SOUTHERN AUSTRALIA'S WARMEST OCTOBER ON RECORD: THE ROLE OF ENSO AND CLIMATE CHANGE

MITCHELL T. BLACK AND DAVID J. KAROLY

*Anthropogenic climate change was found to have a substantial influence on southern Australia's extreme heat in October 2015. The relative influence of El Niño conditions was less clear.*

**Introduction.** Australia experienced its warmest October on record in 2015 (Australian Bureau of Meteorology 2015). This was primarily the result of an early season heat wave in the beginning of the month, concentrated over southern Australia (SAUS; Fig. 23.1a). The monthly anomaly for maximum temperature over SAUS (5.16°C; Fig. 23.1b) was the largest ever recorded for the region for any month of the year. This unseasonably warm weather over SAUS led to an early start to the bushfire season and caused significant crop losses across one of Australia's most important agricultural regions, the Murray–Darling basin.

The October heat coincided with one of the strongest El Niño events on record. While warm and dry conditions over parts of Australia are typical of an El Niño event, the observed record-breaking temperatures may have been exacerbated by climate change. This study uses very large ensembles of atmosphere-only regional climate model simulations to assess the relative roles of the El Niño–Southern Oscillation (ENSO) and anthropogenic climate change in the October 2015 extreme heat across SAUS.

**Data and methods.** Our study made use of the weather@home Australia–New Zealand project (Black et al. 2016) to generate very large ensembles of regional climate model simulations over Australia. This setup uses the atmosphere-only model, HadAM3P, to drive a nested regional model (HadRM3P; 0.44° resolution). For details of the modeling setup, see Black et al. (2016); only a brief description is provided here for context. First, the

model was run under two distinct climate scenarios: observed (all forcings, ALL) and counterfactual (natural forcings only, NAT) realizations of the year 2015. For the ALL simulations, the model was driven by observed sea surface temperatures (SSTs) and sea ice from the Met Office Operational Sea Surface Temperature and Sea Ice Analysis dataset (OSTIA; Donlon et al. 2012), as well as present-day atmospheric composition (well-mixed greenhouse gases, ozone, and aerosols). Very large ensembles were generated by running the model with perturbed initial conditions. For the NAT simulations, the model was driven by preindustrial (1850) atmospheric composition, while the SSTs were modified to remove different estimates of the warming attributable to anthropogenic greenhouse gases. Estimates of the SST changes due to human influence were separately calculated using eight CMIP5 models (Taylor et al. 2012; see online Supplemental Material). Therefore, eight alternative realizations of the NAT climate were created. By adjusting observed SSTs to remove the anthropogenic signal, the main modes of natural variability represented in the ALL SSTs (e.g., the phase of ENSO) are maintained in the NAT climate realizations. Therefore, any change of likelihood of heat events between the ALL and NAT scenarios can be directly attributed to anthropogenic forcing.

To assess the influence of ENSO on the occurrence of SAUS temperature records, additional simulations were generated by driving the weather@home model with composite SST patterns representative of each of the three phases of ENSO: El Niño, Neutral, and La Niña (see online supplemental material for details). Each of these three phases was modeled under both ALL and NAT climate realizations (as per the 2015 runs listed above). Previous work has shown that the weather@home model is able to correctly represent ENSO teleconnections over Australia (Black et al. 2016). We used all of the model simulations that

**AFFILIATIONS:** BLACK AND KAROLY—School of Earth Sciences and ARC Centre of Excellence for Climate System Science, The University of Melbourne, Melbourne, Australia

DOI:10.1175/BAMS-D-16-0124.1

A supplement to this article is available online (10.1175/BAMS-D-16-0124.2)

were available at the time of this writing: at least 2700 members for each of the ALL scenarios (i.e., 2015 ALL, El Niño ALL, Neutral ALL, and La Niña ALL) and at least 650 members for each of the corresponding eight NAT realizations.

For brevity, this study focuses on SAUS because this region experienced exceptional October heat (Fig. 23.1a). A subset of SAUS, the Murray–Darling basin (MDB), is also examined as it is located in the east where the ENSO relationship with temperature is typically stronger (e.g., Min et al. 2013). Homogeneous temperature records for both regions were provided by the Australian Bureau of Meteorology (Figs. 23.1b,c), calculated from the Australian Climate Observations Reference Network–Surface Air Temperature (ACORN-SAT) dataset (Trewin 2013). For both SAUS and the MDB, area-weighted October average maximum temperatures were calculated for each of the ALL and NAT model simulations. As per Black et al. (2015), we correct for model bias (0.13°C for SAUS and 0.68°C for MDB) by adjusting the mean of the NAT distribution to equal that of the early ACORN-SAT observations (1910–39); this bias adjustment is then applied to the ALL distribution.

In line with other common approaches, we define an anomaly threshold based on the previous observed record (+3.68°C for SAUS and +4.15°C for the MDB, both set in 2014; see Figs. 23.1b,c). To quantify the change in risk of extreme heat due to different forcing scenarios, we calculate the fraction of attributable risk (FAR; Allen 2003), defined as  $FAR = 1 - (P_1 / P_2)$ , where  $P_1$  and  $P_2$  represent the probabilities of exceeding the October temperature threshold in two different scenarios. In the first instance, we estimate the anthropogenic influence by setting  $P_1$  to be the probability of exceeding the October temperature threshold in the 2015 NAT scenarios, while  $P_2$  is the equivalent for the 2015 ALL scenario. Here, we aggregate the eight NAT realizations in order to calculate a best estimate of FAR. This process is repeated for the El Niño NAT and El Niño ALL

scenarios. Next, to estimate the influence of El Niño conditions on the change in risk of extreme heat, we calculate FAR using  $P_1$  from the La Niña ALL simulations and  $P_2$  from the El Niño ALL simulations; this is also repeated for Neutral ALL ( $P_1$ ) and El Niño ALL ( $P_2$ ). Therefore, we are able to quantify the change in risk due to both anthropogenic forcing and the phase of ENSO. An assessment of FAR uncertainty was estimated by a bootstrap procedure (10 000 times with replacement) and the 10th percentile FAR value is used to make conservative estimates of changes in

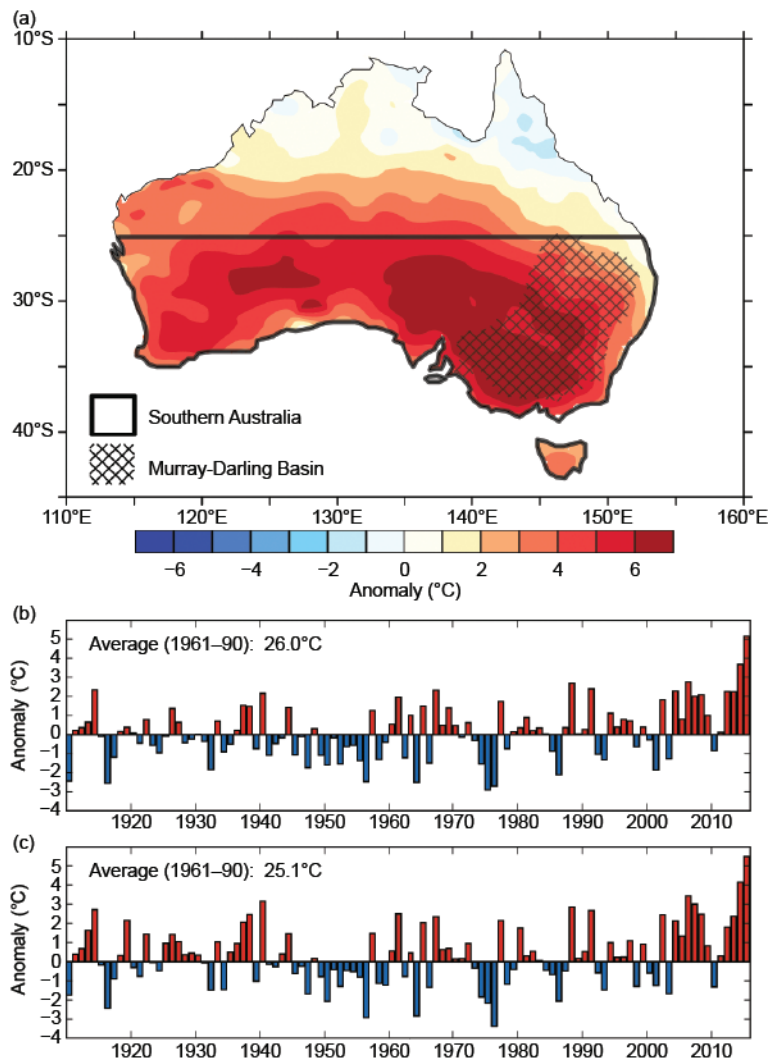


**FIG. 23.1.** Oct mean daily maximum temperatures from °Cthe Australian Bureau of Meteorology, expressed as anomalies relative to the 1961–90 base period. (a) Spatial anomaly field for Oct 2015. The southern Australian region (land area south of 25°S) and the Murray–Darling basin (hatched region) are shown. (b) Timeseries of the southern Australian anomalies from 1910 to 2015, calculated from the Australian Climate Observations Reference Network–Surface Air Temperature dataset (Trewin 2013). (c) As in (b), but for the Murray–Darling basin.

risk associated with the different forcing scenarios. To assist with the interpretation of results, FAR values are also presented as estimated increase in likelihood.

**Results.** Figure 23.2a shows the model-derived distributions of SAUS October average maximum temperature for the various forcing scenarios. There is close agreement between the distributions for the 2015 ALL and El Niño ALL scenarios, as well as between the 2015 NAT and El Niño NAT scenarios, suggesting that the El Niño composite SSTs are a suitable analogue for the 2015 observed conditions. Even though the SSTs for the 2015 El Niño were extreme, the model results in Fig. 23.2a indicate that the associated temperature

anomalies in Australia were consistent with a typical El Niño event. The ALL scenarios are clearly warmer than the NAT scenarios. The La Niña ALL distribution is notably cooler than both Neutral ALL and El Niño ALL, although the warm tails of the distributions are seen to converge. Figure 23.2a suggests that even under La Niña conditions, extreme SAUS and MDB temperatures as warm as in El Niño ALL and Neutral ALL can be achieved.

The corresponding FAR estimates for exceeding the previous SAUS temperature record are shown in Fig. 23.2b. When comparing the ALL scenarios against the NAT scenarios (first two columns of Fig. 23.2b), the 10th percentile FAR estimates are around

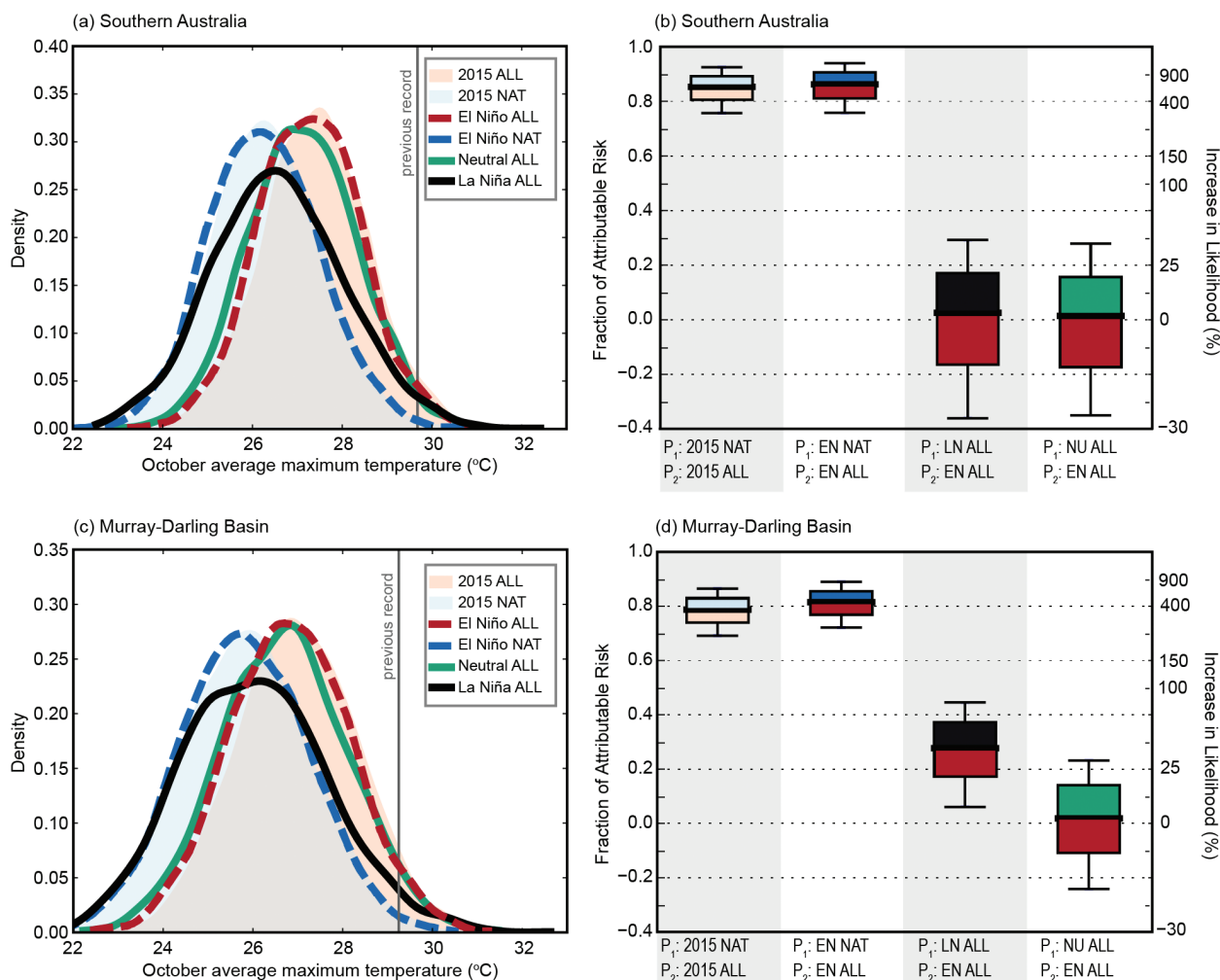


**FIG. 23.2. (a) Distributions of southern Australian Oct average maximum temperatures for the various weather@home modeling scenarios. The vertical line represents the previous temperature record (set in 2014). (b) Corresponding fraction of attributable risk (FAR =  $1 - P_1 / P_2$ ) calculated using different scenario combinations for  $P_1$  and  $P_2$ , as indicated. Estimates of FAR are calculated using a bootstrapping approach (resampling distributions 10000 times with replacement); boxes show the median and interquartile range while the whiskers extend to the 10th and 90th percentiles. See text for details. (c), (d) As in (a), (b) but for the Murray-Darling basin. Abbreviations: El Niño (EN), La Niña (LN), neutral (NU), all forcings (ALL), and natural forcings only (NAT).**

0.76. Therefore, it is very likely (with 90% confidence) that anthropogenic climate change increased the likelihood of breaking the previous SAUS temperature record by at least 400%. Meanwhile, FAR estimates comparing El Niño ALL against La Niña ALL (third column) and Neutral ALL (fourth column) result in the 10th percentiles being below zero. Therefore, we cannot conclude (with 90% confidence) that El Niño conditions increased the likelihood of setting a new SAUS temperature record. The results for the MDB (Figs. 23.2c,d) are similar to SAUS. When comparing the ALL and NAT scenarios for the MDB, the 10th percentile FAR values were of the order of 0.67, that is a 300% increase in likelihood due to anthropogenic climate change. Meanwhile, the ENSO response is clearer over the MDB than for all of SAUS: FAR estimates when comparing El Niño ALL and La Niña ALL indicate it is very likely that El Niño conditions increased the likelihood of breaking the previous MDB record by 4% when compared to La Niña conditions.

**Conclusions.** This study demonstrates a novel approach for separating the role of ENSO and anthropogenic climate change within the context of an event attribution study. Using regional climate model simulations from the weather@home modeling setup, we identify that anthropogenic climate change had a substantial influence on southern Australia's extreme heat in October 2015. El Niño also contributed to the heat, but its relative influence was much weaker. These conclusions, of course, rely heavily on our assumption that our model is able to correctly represent extreme temperatures in southern Australia during El Niño events. However, this cannot be thoroughly tested due to a lack of observational samples. By generating an extremely large number of regional climate model simulations under different forcing scenarios, weather@home is shown to be a powerful tool for understanding the drivers of recent Australian temperature extremes.

**ACKNOWLEDGEMENTS.** The authors have been supported by funding from the Australian Research Council's Centre of Excellence for Climate System Science (Grant CE110001028). Weather@home ANZ is a collaboration between the University of Oxford, the Met Office, the ARC Centre of Excellence for Climate System Science in Australia, NIWA in New Zealand, the University of Melbourne, the University of Tasmania, and the Tasmanian Partnership for Advanced Computing. We thank the volunteers who donated their computing time to run weather@home.

## REFERENCES

- Allen, M., 2003: Liability for climate change. *Nature*, **421**, 891–892, doi:10.1038/421891a.
- Australian Bureau of Meteorology, 2015: Special climate statement 48: Australia's warmest October on record. Bureau of Meteorology, 25pp. [Available online at [www.bom.gov.au/climate/current/statements/scs52.pdf](http://www.bom.gov.au/climate/current/statements/scs52.pdf).]
- Black, M. T., D. J. Karoly, and A. D. King, 2015: The contribution of anthropogenic forcing to the Adelaide and Melbourne, Australia, heat waves of January 2014 [in Explaining Extreme Events of 2014 from a Climate perspective]. *Bull. Amer. Meteor. Soc.*, **96** (12), S145–S148, doi:10.1175/BAMS-D-15-00097.1.
- , and Coauthors, 2016: The weather@home regional climate modelling project for Australia and New Zealand. *Geosci. Model Dev.*, **9**, 3161–3176, doi:10.5194/gmd-9-3161-2016.
- Donlon, C. J., M. Martin, J. Stark, J. Roberts-Jones, E. Fiedler, and W. Wimmer, 2012: The Operational Sea Surface Temperature and Sea Ice Analysis (OSTIA) system. *Remote Sens. Environ.*, **116**, 140–158, doi:10.1016/j.rse.2010.10.017.
- Min, S. K., W. Cai, and P. Whetton, 2013: Influence of climate variability on seasonal extremes over Australia. *J. Geophys. Res. Atmos.*, **118**, 643–654, doi:10.1002/jgrd.50164.
- Taylor, K. E., R. J. Stouffer, and G. A. Meehl, 2012: An overview of CMIP5 and the experiment design. *Bull. Amer. Meteor. Soc.*, **93**, 485–498, doi:10.1175/BAMS-D-11-00094.1.
- Trewin, B., 2013: A daily homogenized temperature data set for Australia. *Int. J. Climatol.*, **33**, 1510–1529, doi:10.1002/joc.3530.